

Adsorption of a fluid in an aerogel: integral equation approach

V. Krakoviack*, E. Kierlik, M.-L. Rosinberg and G. Tarjus

Laboratoire de Physique Théorique des Liquides, Université Pierre et Marie Curie,

4 Place Jussieu, 75252 Paris Cedex 05, France

(November 12, 2018)

Abstract

We present a theoretical study of the phase diagram and the structure of a fluid adsorbed in high-porosity aerogels by means of an integral-equation approach combined with the replica formalism. To simulate a realistic gel environment, we use an aerogel structure factor obtained from an off-lattice diffusion-limited cluster-cluster aggregation process. The predictions of the theory are in qualitative agreement with the experimental results, showing a substantial narrowing of the gas-liquid coexistence curve (compared to that of the bulk fluid), associated with weak changes in the critical density and temperature. The influence of the aerogel structure (nontrivial short-range correlations due to connectedness, long-range fractal behavior of the silica strands) is shown to be important at low fluid densities.

I. INTRODUCTION

The thermodynamics of fluids imbibed in disordered porous materials is a subject of great interest, both from an experimental and from a theoretical perspective [1]. Of special importance is the question of fluid-fluid phase transitions which are found experimentally to be drastically altered compared to the bulk situation. One of these transitions is the so-called capillary condensation observed during the adsorption of a single-component gas at low temperature. It is marked by a steep increase in the adsorbed mass that usually occurs at some pressure below the saturated vapor pressure of the bulk gas.

From an experimental point of view, one has to distinguish two types of systems. A first class of adsorbents consists of mesoporous materials of low porosity (between 30 and 60%), like porous glasses and silica gels. Inside such a matrix, capillary condensation is usually accompanied by a pronounced hysteresis loop that shrinks and eventually disappears at some temperature T_h less than T_c , the bulk critical temperature. This (reproducible) hysteresis loop prevents the direct observation of a thermodynamic, equilibrium phase transition, and the mere existence of a true phase transition underlying capillary condensation in these systems remains a controversial issue. The situation appears clearer for a second class of

*Present address: Department of Chemistry, University of Cambridge, Lensfield Road, Cambridge CB2 1EW, United Kingdom

adsorbents, namely very dilute silica networks like aerogels with porosities as high as 95–98% [2–4]. There is indeed experimental evidence that fluids in such media undergo true phase transitions that terminate at a genuine critical point. Despite the very low density of the adsorbing solids, these transitions display features strikingly different from those of bulk fluids. Thus, the phase diagrams of ^4He and N_2 in aerogels show a marked narrowing of the liquid-vapor coexistence curve and a displacement of the critical point to a lower temperature and a higher density compared to that in the bulk [3]. A similar behavior has been observed for a mixture of isobutyric acid and water in a very dilute silica gel [4].

Recently, the study of a disordered lattice-gas model by means of mean-field density functional theory has provided new insight into the physical origin of the phenomenology associated with capillary condensation [5]. First, it has been found that true equilibrium phase transitions may occur only when the perturbation induced by the solid is sufficiently small. It is thus likely that true phase transitions may occur in aerogels, but not in dense matrices of low porosity. Secondly, it has been shown that hysteresis can occur with or without an underlying phase transition and that, if a transition exists, the disappearance of the hysteresis loop is not associated to capillary criticality. This results from the fact that there is a range of temperature and chemical potential for which the system has many metastable states ; it relies on the assumption, expected to be valid for low-porosity solids, but not necessarily for very dilute gels, that the fluid is not able to fully equilibrate after a change in chemical potential (or pressure).

In the last few years, the concept of “quenched-annealed” binary mixture has been widely used to study the structure and the phase behavior of fluids adsorbed in disordered porous matrices. In this approach, pioneered by Madden and Glandt [6] and further developed by the application of the replica method [7,8], the fluid molecules equilibrate in a matrix of particles frozen in a disordered configuration that is sampled from a given probability distribution. On this basis, computer simulations and integral-equation theories using extensions of standard liquid-state approximations have been proposed [9]. But when the physics of adsorption is dominated by the existence of many metastable states (as shown in Ref. [5]), it is expected that these methods, that have proved very efficient in dealing with bulk fluids and fluids in simple external potentials, could run into difficulties and overestimate the possibility of true phase transitions.

The case of very dilute silica gels is the most likely exception in which these approaches could remain fully operational. Accordingly, we report in the present paper an investigation of the phase behavior of a simple fluid adsorbed in an aerogel within the framework of the integral-equation theory of quenched-annealed binary mixtures. This study is based on the optimized cluster theory (OCT) approach [10] whose application to quenched-annealed mixtures was first considered in Ref. [11]. It can be considered as an extension of previous work toward a description of the actual experimental systems, since, at variance with previous studies of quenched-annealed mixtures, a more realistic model of the solid is used. Indeed, aerogels display very specific structural properties that may play an important role for fluid adsorption. In the past, this has motivated the development of various lattice models taking into account all or part of the specific features of the aerogel-induced disorder ; the phase transitions of these models have been studied by various methods, both theoretically and by computer simulation [12–16]. The present work relies on the off-lattice version [17] of the model used in Refs. [15,16], where the aerogel was described as a connected cluster of sites

generated by a diffusion limited cluster-cluster aggregation (DLCA) process [18,19].

In the next section, the theoretical framework used in this paper is summarized. In section III, the molecular model for the fluid and the matrix are presented, and different aspects of the calculation are discussed. The results are given and discussed in section IV.

II. THEORY

In this section, we first summarize the theoretical expressions on which the present calculation is based. The reader is referred to the original papers for details [11]. We then present and discuss the extension of the formalism needed to treat the problem at hand.

The replica-symmetric Ornstein-Zernike (RSOZ) equations relating the total pair correlation functions $h_{\alpha\beta}(r)$ of a quenched-annealed mixture to the corresponding direct correlation functions $c_{\alpha\beta}(r)$ have been first obtained by Given and Stell [7] and read:

$$h_{00} = c_{00} + \rho_0 c_{00} \otimes h_{00}, \quad (1a)$$

$$h_{10} = c_{10} + \rho_0 c_{10} \otimes h_{00} + \rho_1 c_c \otimes h_{10}, \quad (1b)$$

$$h_{11} = c_{11} + \rho_0 c_{10} \otimes h_{01} + \rho_1 c_c \otimes h_{11} + \rho_1 c_b \otimes h_c, \quad (1c)$$

$$h_c = c_c + \rho_1 c_c \otimes h_c, \quad (1d)$$

where the indices 0 and 1 refer to the matrix and fluid particles respectively, \otimes denotes a convolution, and the indices c and b denote the so-called connected and blocking (or disconnected) parts of h_{11} and c_{11} that obey

$$h_{11} = h_b + h_c, \quad (2)$$

$$c_{11} = c_b + c_c. \quad (3)$$

The replica OCT [11] is applicable to systems with pairwise additive interaction potentials and relies on the separation of these potentials $w_{\alpha\beta}(r)$ into a (repulsive) part $u_{\alpha\beta}^R(r)$ and a perturbative contribution $u_{\alpha\beta}(r)$. The properties of the so-called reference system, in which particles interact through the reference potentials, are assumed to be known, and the central quantities of the theory are then renormalized potentials denoted as $\mathcal{C}_{\alpha\beta}(r)$. Following Ref. [11], we quote here the equations obtained when only hard-sphere reference potentials with diameters $\sigma_{\alpha\beta}$ are considered and when the matrix particles interact with each other only through such a hard-core interaction (i.e., $w_{00}(r) = u_{00}^R(r)$).

The renormalized potentials can be defined through the replica optimized random-phase approximation (ORPA) closure which reads ($\beta = 1/(k_B T)$ where k_B is Boltzmann's constant and T is the temperature)

$$c_{00}(r) = c_{00}^R(r) \quad \text{for } r > \sigma_{00}, \quad (4a)$$

$$c_{10}(r) = c_{10}^R(r) - \beta u_{10}(r) \quad \text{for } r > \sigma_{10}, \quad (4b)$$

$$c_{11}(r) = c_{11}^R(r) - \beta u_{11}(r) \quad \text{for } r > \sigma_{11}, \quad (4c)$$

$$c_b(r) = c_b^R(r), \quad (4d)$$

complemented with the core conditions for the pair distribution functions

$$g_{00}(r) = 0 \quad \text{for } r < \sigma_{00}, \quad (5a)$$

$$g_{10}(r) = 0 \quad \text{for } r < \sigma_{10}, \quad (5b)$$

$$g_{11}(r) = 0 \quad \text{for } r < \sigma_{11}, \quad (5c)$$

(there is no core condition for $g_b(r) = h_b(r) + 1$). Then, one has for the renormalized potentials:

$$\mathcal{C}_{10}(r) = h_{10}(r) - h_{10}^R(r), \quad (6a)$$

$$\mathcal{C}_{11}(r) = h_{11}(r) - h_{11}^R(r), \quad (6b)$$

$$\mathcal{C}_b(r) = h_b(r) - h_b^R(r). \quad (6c)$$

The ORPA free energy of the quenched-annealed system can be determined in a closed form as

$$\begin{aligned} \overline{\mathcal{A}}_{\text{ORPA}} = -\frac{\beta \overline{A}_{\text{ex}}}{V} = & \overline{\mathcal{A}}^R + \frac{1}{2} [\rho_1^2 (\hat{c}_c(0) - \hat{c}_c^R(0)) + 2\rho_1\rho_0 (\hat{c}_{10}(0) - \hat{c}_{10}^R(0))] - \frac{\rho_1}{2} [c_{11}(0) - c_{11}^R(0)] \\ & - \frac{1}{2(2\pi^3)} \int d\mathbf{k} \{ \ln[1 - \rho_1 \hat{c}_c(k)] - \frac{\rho_1}{1 - \rho_1 \hat{c}_c(k)} [\hat{c}_b^R(k) + \rho_0 \frac{\hat{c}_{01}(k)^2}{1 - \rho_0 \hat{c}_{00}(k)}] \} \\ & + \frac{1}{2(2\pi^3)} \int d\mathbf{k} \{ \ln[1 - \rho_1 \hat{c}_c^R(k)] - \frac{\rho_1}{1 - \rho_1 \hat{c}_c^R(k)} [\hat{c}_b^R(k) + \rho_0 \frac{\hat{c}_{01}^R(k)^2}{1 - \rho_0 \hat{c}_{00}(k)}] \}, \end{aligned} \quad (7)$$

or, equivalently, by using the RSOZ equations,

$$\begin{aligned} \overline{\mathcal{A}}_{\text{ORPA}} = & \overline{\mathcal{A}}^R + \frac{1}{2} [\rho_1^2 (\hat{c}_c(0) - \hat{c}_c^R(0)) + \rho_1\rho_0 (\hat{c}_{10}(0) - \hat{c}_{10}^R(0))] - \frac{\rho_1}{2} [c_{11}(0) - c_{11}^R(0)] \\ & - \frac{1}{2(2\pi^3)} \int d\mathbf{k} \ln \frac{1 - \rho_1 \hat{c}_c(k)}{1 - \rho_1 \hat{c}_c^R(k)} - \beta \frac{\rho_1 \rho_0}{2} \int d\mathbf{r} g_{01}(r) u_{01}(r) \\ & + \frac{\rho_1^2}{2} \int d\mathbf{r} [h_c(r) - h_c^R(r)] c_b^R(r) + \frac{\rho_1 \rho_0}{2} \int d\mathbf{r} [h_{01}(r) - h_{01}^R(r)] c_{01}^R(r), \end{aligned} \quad (8)$$

where $\overline{\mathcal{A}}^R$ is the free energy of the reference system.

This ORPA free energy corresponds to the so-called energy route, since it satisfies the Gibbs-Helmholtz equation

$$\overline{U}_{\text{ex}} = \left. \frac{\partial \beta \overline{A}_{\text{ex}}}{\partial \beta} \right|_{V, \rho_0}, \quad (9)$$

where \overline{U}_{ex} is the configurational internal energy of the fluid inside the matrix and is given by

$$\frac{\overline{U}_{\text{ex}}}{V} = \frac{1}{2} \int d\mathbf{r} [\rho_1^2 g_{11}(r) u_{11}(r) + 2\rho_1 \rho_0 g_{01}(r) u_{01}(r)]. \quad (10)$$

The mean-spherical approximation (MSA) is obtained from the ORPA when the reference system is described by the Percus-Yevick (PY) approximation, which corresponds to

$$c_{00}^R(r) = 0 \quad \text{for } r > \sigma_{00}, \quad (11a)$$

$$c_{10}^R(r) = 0 \quad \text{for } r > \sigma_{10}, \quad (11b)$$

$$c_{11}^R(r) = 0 \quad \text{for } r > \sigma_{11}, \quad (11c)$$

$$c_b^R(r) = 0 \quad \text{for } r > 0. \quad (11d)$$

Within this latter approximation, an expression for the excess chemical potential can be derived:

$$\begin{aligned} \beta[\mu_{ex} - \mu_{ex}^R] &= \frac{1}{2}[c_{11}(0) - c_{11}^R(0)] - \rho_1[\hat{c}_{11}(0) - \hat{c}_{11}^R(0)] \\ &\quad - \rho_0[\hat{c}_{01}(0) - \hat{c}_{01}^R(0)] \\ &= \frac{\beta}{2} \int d\mathbf{r} [\rho_1 g_{11}(r) u_{11}(r) + \rho_0 g_{01}(r) u_{01}(r)] \\ &\quad - \frac{\rho_1}{2}[\hat{c}_{11}(0) - \hat{c}_{11}^R(0)] - \frac{\rho_0}{2}[\hat{c}_{01}(0) - \hat{c}_{01}^R(0)]. \end{aligned} \quad (12)$$

As is often the case with simple closures, both the ORPA and the MSA are thermodynamically inconsistent, which means that the free energy obtained from the above energy route differs from that obtained by integration with respect to the fluid density of the compressibility equation [8,20]

$$\frac{\beta}{\rho_1 \chi} = 1 - \rho_1 \hat{c}_c(0), \quad (13)$$

where χ is the isothermal compressibility of the fluid inside the matrix. This is an important remark, since it turns out that the compressibility route does not yield a critical point in 3 dimensions [21], whereas the energy route provides one, albeit with an associated classical (mean-field) behavior.

Finally, by truncating the OCT diagrammatic expansion to the first order beyond ORPA, one obtains the ORPA+B2 approximation for the free energy [11], that is the sum of the ORPA result, Eq. (9), and of the corrective term

$$\begin{aligned} B_2 &= \frac{1}{2} \rho_1 \rho_0 \int d\mathbf{r} h_{01}^R(r) [\mathcal{C}_{01}(r)]^2 + \rho_1 \rho_0 \int d\mathbf{r} g_{01}^R(r) \sum_{n=3}^{\infty} \frac{1}{n!} [\mathcal{C}_{01}(r)]^n \\ &\quad + \frac{1}{4} \rho_1^2 \int d\mathbf{r} h_{11}^R(r) [\mathcal{C}_{11}(r)]^2 + \frac{1}{2} \rho_1^2 \int d\mathbf{r} g_{11}^R(r) \sum_{n=3}^{\infty} \frac{1}{n!} [\mathcal{C}_{11}(r)]^n \\ &\quad - \frac{1}{4} \rho_1^2 \int d\mathbf{r} h_b^R(r) [\mathcal{C}_b(r)]^2 - \frac{1}{2} \rho_1^2 \int d\mathbf{r} g_b^R(r) \sum_{n=3}^{\infty} \frac{1}{n!} [\mathcal{C}_b(r)]^n. \end{aligned} \quad (14)$$

The associated EXP approximation for the pair distribution functions is given by [11]

$$g_{01}^{EXP}(r) = g_{01}^R(r) \exp[\mathcal{C}_{01}(r)] \quad (15a)$$

$$g_{11}^{EXP}(r) = g_{11}^R(r) \exp[\mathcal{C}_{11}(r)], \quad (15b)$$

$$g_b^{EXP}(r) = g_b^R(r) \exp[\mathcal{C}_b(r)], \quad (15c)$$

$$g_c^{EXP}(r) = g_{11}^{EXP}(r) - g_b^{EXP}(r). \quad (15d)$$

A noticeable property of the above equations describing the structure and the thermodynamics of a fluid adsorbed in a disordered matrix is that the quenched matrix enters solely through its pair correlation function $h_{00}(r)$. The basic strategy followed in this paper is to take advantage of this property to study fluid adsorption in a model aerogel obtained by an out-of-equilibrium aggregation process (see below). The aerogel is then only characterized by its pair distribution function (in fact, its structure factor obtained by Fourier transform) determined by computer simulation. At first sight, this may lead to a conceptual difficulty. Indeed, the original treatment of quenched-annealed mixtures was restricted to situations in which the matrix is obtained by quenching an equilibrium distribution [6–8]. However, as was stressed by Madden [22], there is no such difficulty and the RSOZ equations apply in a more general context, although the diagrammatic structure of the direct correlation functions is non-standard (indeed, these equations simply follow from the Legendre transform that relates the generating functional of the total correlation functions to the generating functional of the direct correlation functions). One can use the OCT approximation scheme as well.

III. MODEL SYSTEMS AND NUMERICAL METHODS

As stressed above, aerogels display very specific structural properties that can be expected to have a strong influence on the properties of the adsorbed fluids. First, they are made of long chains of connected, almost spherical, colloidal SiO_2 particles. Despite the very low density of the adsorbent, this connectedness induces short-range correlations that differ from that generated by equilibrium hard-sphere matrices. Secondly, the silica strands forming the gel are organized into a long-range, fractally correlated structure whose experimental signature is a pronounced peak at small wave-vectors in the intensities measured by small-angle x-ray or neutron scattering. Accordingly, it seems important to use a modeling of the aerogel structure that reproduces these two properties. In the present work, the aerogel is modeled as a connected cluster of spheres generated by a diffusion-limited cluster-cluster aggregation (DLCA) process [18,19]. This process mimics the mechanisms involved in the synthesis of real aerogels, and the three-dimensional off-lattice version used here has been shown to provide gel structures that correctly account for both the short-range and long-range structural properties of real silica aerogels [17].

For a given matrix density ρ_0 , the only information about the matrix that is needed in our calculation is the sample averaged structure factor $S_{00}(q)$ defined from the averaged pair correlation function $h_{00}(r)$ as

$$S_{00}(q) = 1 + \rho_0 \int_0^\infty h_{00}(r) \frac{\sin(qr)}{qr} 4\pi r^2 dr.$$

$S_{00}(q)$ has been computed following the lines of the original work of Hasmy *et al.* [17] and the reader is referred to the corresponding publications for details. The corresponding curves for the three densities studied in this work ($\rho_0 = 0.025, 0.05, 0.1$) are reported in Fig. 1. Two characteristic features of aerogel structures are clearly seen on these data: at large q ($q\sigma_{00} > 2\pi$), one finds for all densities

$$S_{00}(q) \simeq 1 + 2 \frac{\sin(q\sigma_{00})}{q\sigma_{00}},$$

which corresponds to the fact that each aerogel particle has on average two neighbors connected to it, whereas at low q ($q\sigma_{00} < 2$), a broad peak whose amplitude increases as density decreases is found, that originates from the long-range, fractal correlations of the particle strands forming the material.

The matrix-fluid and fluid-fluid interactions are split into a hard-sphere part and a Lennard-Jones 12-6 tail following Weeks, Chandler and Andersen [23], i.e., $u_{\alpha\beta}(r) = -\varepsilon_{\alpha\beta}$ for $\sigma_{\alpha\beta} < r < 2^{1/6}\sigma_{\alpha\beta}$ and $u_{\alpha\beta}(r) = 4\varepsilon_{\alpha\beta}[(\sigma_{\alpha\beta}/r)^{12} - (\sigma_{\alpha\beta}/r)^6]$ for $r > 2^{1/6}\sigma_{\alpha\beta}$. The use of hard-sphere cores for all the repulsive potentials is chosen to avoid difficulties associated with calculating the free energy of fluids with soft-core repulsive forces. Moreover, the Lennard-Jones tails are truncated at $r/\sigma_{\alpha\beta} = 2.5$.

In order to make contact with previous work [11], we have only considered systems in which all particles have the same diameter, i.e., $\sigma_{00} = \sigma_{01} = \sigma_{11} = \sigma$. It has to be stressed that this choice is rather unrealistic with respect to the actual experimental situation, since the silica particles forming the aerogels are always much larger than the adsorbate (typically, by a factor of ten). However, the model captures most of the specific nature of the correlated disorder induced by an aerogel and this is expected to be sufficient to give an account of the generic experimental behavior. Like in previous studies, we introduce the interaction ratio $y = \varepsilon_{01}/\varepsilon_{11}$, and, in the following, σ will be used as the length unit, ε_{11} as the energy unit and ε_{11}/k_B as the temperature unit.

In all calculations, the correlation functions of the reference system were obtained by solving the RSOZ equations in the Percus-Yevick approximation and the corresponding pressure and chemical potential were obtained by integration of the compressibility equation of state, Eq. (13). This is an additional approximation in the ORPA+B₂/EXP framework. However, we know from previous studies [9] that the PY theory gives a good description of the reference-system properties when matrix and fluid particles have the same size. However, because these previous studies have dealt only with matrices quenched from an equilibrium distribution, we have tried to obtain another assessment of this approximation for the present situation of an “out-of-equilibrium” matrix by computing the Henry’s constant K_H of the reference system. For a hard-sphere system, K_H is simply the fraction of the total volume of the matrix that is accessible to the center of a single adsorbate molecule. Thus, we have first estimated K_H by direct Monte-Carlo integration for various realizations of the model aerogels at the three working densities. Then, we have computed the theoretical value by using the (scaled-particle-theory) charging process expression (remembering that $K_H = \exp[-\beta\mu_{ex}^R(\rho_1 = 0)]$),

$$K_H = \exp \left(-\rho_0 \int_0^\sigma G_{01}(r; r; \rho_1 = 0) 4\pi r^2 dr \right),$$

where $G_{01}(r; r; \rho_1 = 0)$ is the contact value at zero adsorbate density of the fluid-matrix pair distribution function when the corresponding hard-core diameter equals r [24]. The value of $G_{01}(r; r; \rho_1 = 0)$ is determined in the Percus-Yevick approximation for various values of r between 0 and σ and the integral is estimated as a discrete sum. Note that a similar calculation has already been proposed by Ford *et al.* [25] and appeared to be quite successful. The results of both estimations are reported in table I and show a very good agreement, thereby confirming the accuracy of the PY description of the reference system.

In order to solve the RSOZ equations, we used Gillan’s method [26] with a grid size of 0.02σ and 16384 points in most of the calculations. Once the correlation functions were

obtained, we deduced the renormalized potentials and computed the free energy to the chosen approximation. In order to calculate the phase diagram of the fluid inside the matrix, series of adsorption isotherms μ vs ρ_1 were generated. When the curve had a loop, similar to those seen in the van der Waals theory of equilibrium fluids, the densities ρ'_1 and ρ''_1 of the two coexisting phases were determined by solving the system of equations

$$P(\rho'_1) = P(\rho''_1), \quad \mu(\rho'_1) = \mu(\rho''_1),$$

where $P = -\partial\bar{A}/\partial V|_{T,\rho_0}$ is the grand potential density (or thermodynamic pressure of the fluid [8]).

In Ref. [11], it was shown that there is a great sensitivity of the calculated phase diagrams to the approximations used in the theory. This is the case in the present calculation as well, as can be seen in Fig. 2, where the MSA and ORPA+B2 phase diagrams are compared for typical values of the parameters. Note that the fluid density has been normalized by the porosity of the matrix that is equal to $1 - \eta_0$, where $\eta_0 = \pi\rho_0\sigma^3/6$ is the corresponding packing fraction. In the following, we will concentrate on the results of the ORPA+B2/EXP approximation. There are two motivations to this choice. The first one is of fundamental nature. Experiments show unambiguously that it is the low-density part of the phase diagram that is the most strongly affected by the presence of an aerogel. So, it is sensible to address the problem with a theory well adapted to this low-density regime. For bulk fluids, it is well known that, at variance with the lower-order approximations ORPA or MSA, the ORPA+B2 theory predicts the free energy with the same level of accuracy in the low-density gas and the high-density liquid phases and that the EXP approximation gives the exact low-density limit for the pair distribution functions [10]. This is not true anymore when one considers quenched-annealed system (for instance, the ORPA+B2 free energy does not yield in general the exact second virial coefficient for the fluid inside the matrix, because the term of order ρ_1^2 contains contributions from all orders in ρ_0), but one still expects that the ORPA+B2/EXP theory will remain accurate in the case of a low-density gas adsorbed in a low-density matrix. The second reason is more pragmatic and comes from the comparison with the simulation results of Álvarez *et al.* [27] for hard-sphere matrices of low and moderate densities. In this case, the ORPA+B2 phase diagrams turn out to give the best agreement with the simulation results. This is shown in Fig. 3, where the simulation results tabulated in Ref. [27] are compared with the theoretical curves of Ref. [11]: the agreement is reasonably good (much better indeed than with MSA).

IV. RESULTS

We first present the results for the structure of the adsorbed fluid, since it shows remarkable features originating in the specific properties of the aerogel, in particular its connectedness.

The first effect of the aerogel structure shows up already in the case of purely repulsive matrix-fluid interactions ($y = 0$). This is illustrated in Fig. 4, where the matrix-fluid correlation function $g_{01}(r)$ at gas density ($\rho_1 = 0.02$) displays a very clear depletion near contact. This “correlation hole” comes from the presence of a region surrounding each matrix particle from which the adsorbate molecules are excluded. This region disappears

when density is increased, as can be seen from the $g_{01}(r)$ at liquid density ($\rho_1 = 0.70$). This correlation hole, as well as the accompanying cusp at $r/\sigma = 2$, is a well-known feature of molecular systems made of tangentially jointed hard-spheres, like our model aerogel. For instance, it has been found in fluids of freely-jointed hard-sphere chains, by both computer simulation and theory [28]. It is a simple steric effect due to the presence of the neighboring beads that hinders the approach of a gas molecule.

The second effect, expected to manifest itself at low enough temperatures when attractive matrix-fluid interactions are turned on, is a much stronger binding of the adsorbate particles to the solid matrix than in the previously investigated models. Indeed, on one hand, two tangent aerogel beads form adsorption sites with potential energy equal or lower than $-2\varepsilon_{01}$ (the direct contribution of the two beads being still lowered by contributions from their neighboring beads); on the other hand, the aerogel structure presents large voids [17,29] in which the adsorption potential energy due to the matrix is zero. This leads to a highly inhomogeneous potential energy field and thus to strong preferential adsorption on the aerogel strands. The situation is very different in the case of an equilibrium hard-sphere matrix at a similar density, as shown by the following simple calculation. For such a matrix at a density $\rho_0 = 0.05$, the average distance between two spheres is roughly $d = (\rho_0)^{-1/3} \simeq 2.7$. If an adsorbate particle is equidistant from two matrix particles, it experiences from these particles a potential energy roughly equal to $2u_{10}(r = d/2) = -1.075 \varepsilon_{01}$, whereas if it is adsorbed on a matrix particle, it experiences a potential energy simply equal to $-\varepsilon_{01}$. The situation is thus far less contrasted than in an aerogel and one expects a relatively weak binding of the adsorbate on the matrix.

This second effect should result in highly inhomogeneous distributions of the fluid particles and is thus difficult to detect from averaged quantities like pair distribution functions. We find nevertheless a few indications of its influence on the adsorbate structure. One of them can be seen in Fig. 5. It is indeed quite direct to see from the values of the pair distribution functions near contact that, at the two vapor densities considered ($\rho_1 = 0.02$ and $\rho_1 = 0.2$), there are roughly twice more adsorbate particles around a matrix particle than around a given adsorbate particle. This is compatible with the picture of the formation of a strongly bound monolayer of particles adsorbed on the aerogel strands. It agrees with the statement by Chan *et al.* that the “gas” phase in very dilute aerogels actually consists of vapor plus a liquid film that coats the random silica strands [3]. This situation differs strongly from that in equilibrium hard-sphere matrices, where the prevailing adsorption mechanism is expected to be the formation of liquids droplets in the denser regions of the matrix. In this latter case, the environments of the matrix and fluid particles are not too different. This is precisely what is found in Ref. [11] (see Fig. 13 of this paper and the related discussion). Another indication of strong adsorption on the aerogel strands is the presence of structural correlations typical of the aerogel structure in the adsorbed low-density phase. Indeed, if the adsorbate particles coat the aerogel strands, it is expected that their distribution will retain part of the spatial arrangement of the substrate, in particular the long-range correlations that show up in the form of a maximum at small wave vectors. To test this idea, we have

calculated the partial structure factors of the system defined as [30]

$$S_{11}^p(q) = \frac{\rho_1}{\rho_0 + \rho_1} (1 + \rho_1 \hat{h}_{11}(q)),$$

$$S_{01}^p(q) = \frac{\rho_0}{\rho_0 + \rho_1} \rho_1 \hat{h}_{01}(q).$$

Results are shown in Fig. 6, where it is clearly seen that a broad correlation peak builds up at small q ($q\sigma \simeq 0.2$) when increasing the vapor density, at a position in good agreement with the position of the corresponding peak in the aerogel structure factor (compare with Fig. 1). This can again be interpreted as evidence for the progressive formation of a thin layer of adsorbed particles coating the gel strands.

These characteristic features of adsorbed fluid phases in aerogels are important at low adsorbate density only. Indeed, as can be seen in Figs. 4 to 6, they are almost completely absent at liquid densities, for which the physics of the system is dominated by the hardcore interaction between adsorbate particles so that the structure of the adsorbent becomes of marginal importance. Thus, these observations stress *a posteriori* the need to use a theoretical framework well adapted to the description of the low-density regime, hence the use of the ORPA+B2/EXP theory in this work. But they also show that the case under study is an especially difficult one in the context of the OCT: indeed, of the two effects discussed above, the first one, that is purely steric in origin, competes with the second one, that is only due to the attractive matrix-fluid interactions.

We now turn to the presentation of the capillary phase diagrams. We only report the results corresponding to the case where both fluid-fluid and matrix-fluid attractive interactions are present, which is the case of experimental relevance.

Fig. 7 shows coexistence envelopes of the fluid phases obtained from the ORPA+B2 approximation as one varies the ratio y for a typical aerogel density $\rho_0 = 0.05$ corresponding to a porosity $1 - \eta_0 = 97.4\%$. It is seen that the variation of the capillary critical temperature with y is non-monotonic: T_{cc} first increases and then decreases as one increases y , the maximum value being found around $y = 1$. On the other hand, the critical density increases monotonically and becomes larger than the bulk value for $y = 1$ (this not due to the normalization by $1 - \eta_0$). The latter behavior agrees with the experimental observation that ρ_{1c} is displaced towards the liquid phase when the interaction with the porous material is sufficiently attractive [3]. Despite the low density of the aerogel, there is also a significant narrowing of the coexistence curves compared to the bulk one when $y > 1$, although this effect is still smaller than that observed in the experiments (see below) [3,4].

Fig. 8 shows the effect of varying the aerogel density at a fixed value of the interaction ratio $y = 1.5$. It is found that the normalized critical density increases only slightly with the matrix density and that the width of the coexistence curve does not vary very much. However, for $y = 1.5$ and $\rho_0 = 0.025$, a “precondensation” transition is obtained, similar to what has already been found in various models [9,11] (see also Maritan *et al.* [31]). A surprising result seen in this figure is the non-monotonic variation of the capillary critical temperature that first increases with ρ_0 and then decreases, leading to the somewhat unexpected result that for a low enough matrix density T_{cc} is larger than its bulk value. The physical origin, if any, of this behavior is unclear to us, but there is *a priori* no fundamental reason forbidding such a behavior. A possible explanation could be the very weak confinement effect due to the dilute gel. Indeed, it is well known, already at the mean-field level,

that confinement induces a lowering of the critical temperature of a fluid. In particular, this is what is found in all cases of simple pore geometries [1]. But aerogels are rather special in this respect: because of their very open structure, they have no real pores with well defined walls. The comparison with the case of equilibrium hard-sphere matrices gives an insight on the potential relevance of this fact. Indeed, in the latter case, it has been found that adsorption partly counterbalances the influence of confinement, so that the lowering of the critical temperatures is less pronounced in the case of attractive fluid-matrix interactions than in the completely repulsive case. A possible origin of our finding for aerogels could thus be that the effect of the attractive matrix-fluid interaction now dominates the very weak influence of confinement.

The remaining question is of course to see how our results based on a realistic description of the structural correlations in an aerogel compare with experiments and with previous results obtained with the less realistic equilibrium hard-sphere model.

As already stated in the introduction, the most significant experimental observation is a marked narrowing of the liquid-vapor coexistence curve relative to that in the bulk, a narrowing that is accompanied by a slight displacement of the critical point to a lower temperature and a higher density. Chan *et al.* [3] have proposed to quantify this narrowing by fitting the top of the coexistence curves for ^4He and N_2 adsorbed in 95% aerogels with the critical expression

$$\frac{\rho_l - \rho_v}{\rho_{1c}} = B \left[\frac{T_{cc} - T}{T_{cc}} \right]^\beta,$$

where ρ_v and ρ_l are, respectively, the vapor and liquid densities of the adsorbed fluid, and they have found that the amplitude factors B are respectively about 14 and 2.6 times smaller than the bulk values for these two fluids (in both cases, the value of the exponent β is consistent with that found for the bulk fluids). These values, which seem indicative of a large reduction of the phase coexistence envelopes, have nevertheless to be taken with care. Indeed, in the case of ^4He , the previous result has been obtained from data in the temperature range 5.15–5.17 K, T_{cc} being found equal to 5.167 K. Further experiments in a wider temperature domain (2.5–5 K) have shown that the reduction of the phase envelope is much more pronounced near the critical point than well below the critical temperature [32]. For instance, when the temperature is roughly $0.64 T_c$, the ratio of the widths of the bulk and adsorbed fluid phase diagrams is not larger than about 2.2.

As can be seen in Figs. 7 and 8, for values of y that are large enough, one finds that our model gives results in good qualitative agreement with the picture emerging from experiments: the critical density is slightly shifted to values higher than in the bulk and, except for the lowest aerogel density, the critical temperature is found to decrease, albeit moderately. A significant narrowing of the coexistence curves is also found. For instance, with $\rho_0 = 0.05$ and $y = 1.5$, the ratio of the widths of the bulk and adsorbed fluid phase diagrams is about 1.4 at $T = 0.8 \simeq 0.65 T_c$ and it increases with y . (However, our present approach is unable to capture the behavior seen in the ^4He experiment in the close vicinity of T_{cc} .)

Figs. 9 (a) and 9 (b) show a comparison between the coexistence curves obtained for a fluid adsorbed in model aerogels and equilibrium hard-sphere matrices. It is seen that, at given matrix density ρ_0 , and ratio of interactions y , the coexistence curves in the case of the model aerogel are always narrower, and the critical temperatures always higher, than in the

equilibrium hard-sphere case. The effect is quite significant for $y = 1.5$, where the ratio of the widths of the bulk and adsorbed fluid phase envelopes is about 90 % at $T = 0.8 \simeq 0.65 T_c$ for hard-sphere matrices, compared to about 70 % for aerogels. Combined with the fact that the width of the coexistence curves varies only weakly with the aerogel density, we thus find that using a more realistic model of the adsorbent makes it possible to obtain a behavior that more closely resembles the experimental one, i.e., a substantial narrowing of the phase envelope associated to weak changes in the critical temperature and density. (It should also be stressed that for the small matrix densities used here, the hard-sphere matrix is far from being a connected medium.) We note however that this improvement of the situation compared to experiments is limited to a certain range of parameters, since the differences between the two types of matrices become rather modest for larger values of y ($y > 2$), for which it seems that the strength of the attractive matrix-fluid potential limits the relevance of the detailed structure of the adsorbent.

V. CONCLUSION

In this paper, we have presented a theoretical study of the phase diagram and the structure of simple fluids adsorbed in high-porosity aerogels. For these systems, the perturbation induced by the adsorbent is *a priori* small, and one expects the integral-equation approach combined with the replica formalism to provide a reasonable description. The novelty of the present work is that a realistic description of the aerogel structure has been incorporated via the use of the static structure factor of model aerogels built from an off-lattice diffusion limited cluster-cluster aggregation process. Unlike cruder models based on quenched configurations of equilibrium hard or penetrable spheres, the correlations between matrix particles at the low density studied (corresponding to porosities between 90% and 97.5%) keep track of the short-range connectedness of the aerogel and of the long-range fractal behavior. The predictions of the theory are in qualitative agreement with the experimental results, showing a significant narrowing of the gas-liquid coexistence curve associated with weak changes in the critical temperature and density. In addition, the influence of the aerogel structure is shown to be important at low fluid densities. Improving the present approach is still needed in two directions: first, to provide a better description of the critical region, but this represents a very challenging task for systems like fluids adsorbed in disordered porous media that are akin to random fields models; secondly, to go one step further toward a realistic modeling of the adsorbent by allowing the beads composing the silica strands of the aerogel to be much larger (typically, by a factor of ten) than the fluid particles. The latter improvement of the description requires both the development of more appropriate closures of the Ornstein-Zernike equations for mixtures of particles with very different sizes and the introduction of a more realistic potential between the matrix and the fluid particles (using for instance the composite-sphere potential proposed in Ref. [33]).

The Laboratoire de Physique Théorique des Liquides is UMR 7600 of the CNRS. We thank R. Jullien for providing us with his DCLA algorithm to build the model aerogels and

M. Chan for communicating unpublished experimental results.

REFERENCES

- [1] For reviews see B. J. Frisken, A. J. Liu, and D. S. Cannell, Mater. Res. Soc. Bull., **29**, 19 (1994); L. D. Gelb, K. E. Gubbins, R. Radhakrishnan, and M. Sliwinska-Bartkowiak, Rep. Prog. Phys. **62**, 1573 (1999).
- [2] B. J. Frisken, F. Ferri, and D. S. Cannell, Phys. Rev. Lett. **66**, 2754 (1991); B. J. Frisken and D. S. Cannell, *ibid.* **69**, 632 (1992); B. J. Frisken, F. Ferri, and D. S. Cannell, Phys. Rev. E **51**, 5922 (1995).
- [3] A. P. Y. Wong and M. H. W. Chan, Phys. Rev. Lett. **65**, 2567 (1990); A. P. Y. Wong, S. B. Kim, W. I. Goldburg, and M. H. W. Chan, *ibid.* **70**, 954 (1993); D. J. Tulimieri, J. Yoon, and M. H. W. Chan, Phys. Rev. Lett. **82**, 121 (1999); L. B. Lurio *et al.*, J. Low Temp. Phys. **121**, 591 (2000).
- [4] Z. Zhuang, A. G. Casielles, and D. S. Cannell, Phys. Rev. Lett. **77**, 2969 (1996).
- [5] E. Kierlik, M. L. Rosinberg, G. Tarjus, and P. Viot, Phys. Chem. Chem. Phys. **3**, 1201 (2001); E. Kierlik, P. Monson, M. L. Rosinberg, L. Sarkisov, and G. Tarjus, Phys. Rev. Lett. **87**, 055701 (2001).
- [6] W. G. Madden and E. D. Glandt, J. Stat. Phys. **51**, 537 (1988); W. G. Madden, J. Chem. Phys. **96**, 5422 (1992).
- [7] J. A. Given, Phys. Rev. A **45**, 816 (1992); J. A. Given and G. Stell, J. Chem. Phys. **97**, 4573 (1992).
- [8] M. L. Rosinberg, G. Tarjus, and G. Stell, J. Chem. Phys. **100**, 5172 (1994); E. Kierlik, P. A. Monson, M.L. Rosinberg, and G. Tarjus, J. Chem. Phys. **103**, 4256 (1995).
- [9] For a review see M.L. Rosinberg, in *New Approaches to Problems in Liquid State Theory*, edited by C. Caccamo, J.-P. Hansen, and G. Stell, NATO Science Series (Kluwer, Dordrecht, 1999).
- [10] H. C. Andersen and D. Chandler, J. Chem. Phys. **57**, 1918 (1972).
- [11] E. Kierlik, M. L. Rosinberg, G. Tarjus, and P. A. Monson, J. Chem. Phys. **106**, 264 (1997); *ibid.* **110**, 689 (1999).
- [12] J. Machta, Phys. Rev. Lett. **66**, 169 (1991).
- [13] D. Stauffer and R. B. Pandey, J. Phys. A **25**, L1079 (1992).
- [14] A. Falicov and A. N. Berker, Phys. Rev. Lett. **74**, 426 (1995); A. Lopatnikova and A. N. Berker, Phys. Rev. B **56**, 11865 (1997).
- [15] K. Uzelac, A. Hasmy, and R. Jullien, Phys. Rev. Lett. **74**, 422 (1995); J. Non-Cryst. Solids **186**, 365 (1995).
- [16] R. Salazar, R. Toral, and A. Chakrabarti, J. Sol-Gel Sci. Technol. **15**, 175 (1999).
- [17] A. Hasmy, M. Foret, J. Pelous, and R. Jullien, Phys. Rev. B **48**, 9345 (1993); A. Hasmy, R. Vacher, and R. Jullien, *ibid.* **50**, 1305 (1994); A. Hasmy, E. Anglaret, M. Foret, J. Pelous, and R. Jullien, *ibid.* **50**, 6006 (1994); A. Hasmy, M. Foret, E. Anglaret, J. Pelous, R. Jullien, and R. Vacher, J. of Non-Cryst. Solids. **186**, 118 (1995).
- [18] P. Meakin, Phys. Rev. Lett. **51**, 1119 (1983).
- [19] M. Kolb, R. Botet, and R. Jullien, Phys. Rev. Lett. **51**, 1123 (1983).
- [20] D. M. Ford and E. D. Glandt, J. Chem. Phys. **100**, 2391 (1994)
- [21] E. Pitard, M. L. Rosinberg, G. Stell, and G. Tarjus, Phys. Rev. Lett. **74**, 4361 (1995).
- [22] W. G. Madden, J. Chem. Phys. **102**, 5572 (1995).
- [23] J. D. Weeks, D. Chandler, and H. C. Andersen, J. Chem. Phys. **54**, 5237 (1971).

- [24] H. Reiss, H. L. Frisch, and J. L. Lebowitz, *J. Chem. Phys.* **31**, 369 (1959); J. L. Lebowitz, E. Helfand, and E. Praestgaard, *ibid.* **43**, 774 (1965).
- [25] D. M. Ford, A. P. Thompson, and E. D. Glandt, *J. Chem. Phys.* **103**, 1099 (1995).
- [26] M. J. Gillan, *Mol. Phys.* **38**, 1781 (1979).
- [27] M. Álvarez, D. Levesque, and J.-J. Weis, *Phys. Rev. E* **60**, 5495 (1999).
- [28] A. Yethiraj, C. K. Hall, and K. G. Honnell, *J. Chem. Phys.* **93**, 4453 (1990); Y. C. Chiew, *ibid.* **93**, 5067 (1990); E. Kierlik and M. L. Rosinberg, *ibid.* **99**, 3950 (1993).
- [29] J. V. Porto and J. M. Parpia, *Phys. Rev. B* **59**, 14583 (1999).
- [30] J. P. Hansen and I. R. McDonald, *Theory of Simple Liquids* (Academic, New York, 1976).
- [31] A. Maritan, M. R. Swift, M. Cieplak, M. H. W. Chan, M. W. Cole, and J. R. Banavar, *Phys. Rev. Lett.* **67**, 1821 (1991).
- [32] M. H. W. Chan, private communication.
- [33] R. D. Kaminsky and P. A. Monson, *J. Chem. Phys.* **95**, 2936 (1991).

TABLES

ρ_0	MC	PY	EHS
0.025	0.934	0.927	0.898
0.05	0.868	0.856	0.802
0.1	0.739	0.718	0.629

TABLE I. Henry's constant of a hard-sphere fluid adsorbed in DLCA aerogels, calculated by direct Monte-Carlo integration (MC) and within the Percus-Yevick approximation (PY) through a scaled-particle-theory charging process. The fluid and matrix particles have the same diameter. For comparison, the values for hard-sphere matrices (EHS) calculated as in Ref. [11] are also given.

FIGURES

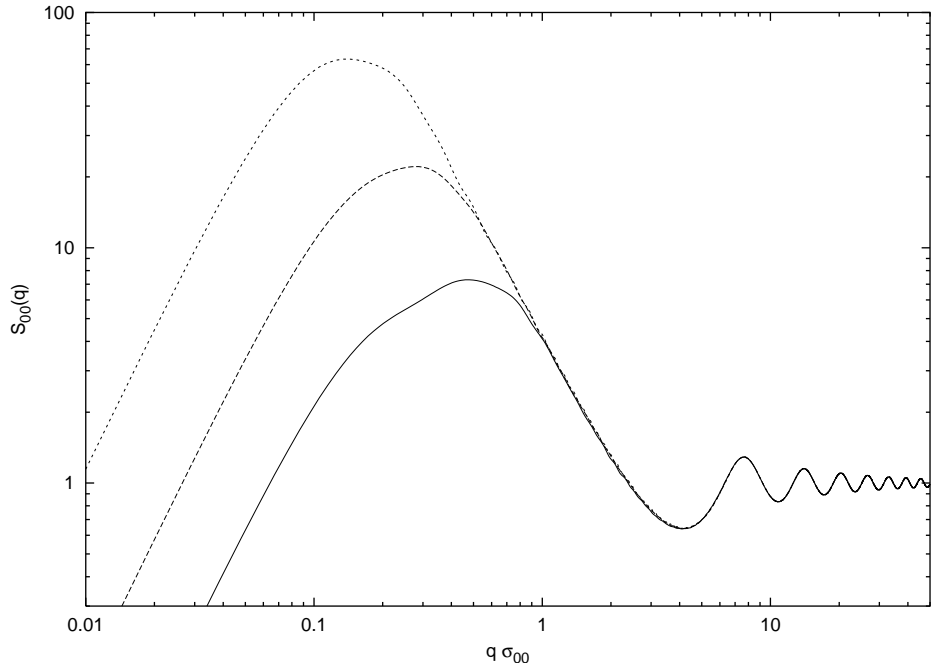


FIG. 1. DLCA aerogel structure factors at three different densities: $\rho_0 = 0.025, 0.05, 0.1$ (from top to bottom). These curves represent averages over 40 realizations of the aerogel generated at a given density.

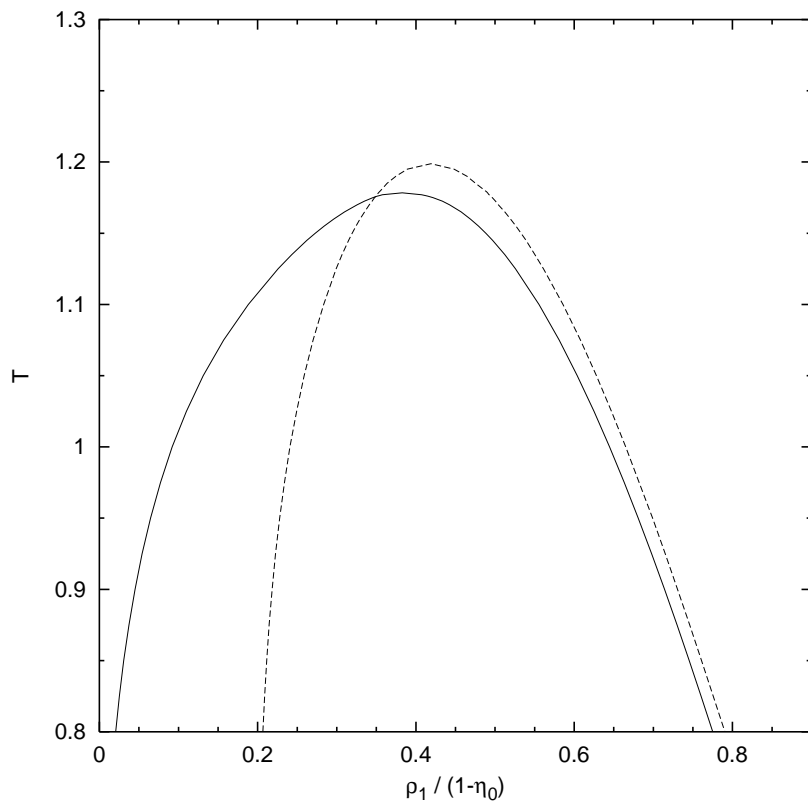


FIG. 2. Comparison of the coexistence envelopes for a fluid confined in an aerogel matrix ($\rho_0 = 0.05$, $y = 1.5$) computed within the MSA (solid line) and the ORPA+B2 (dashed line).

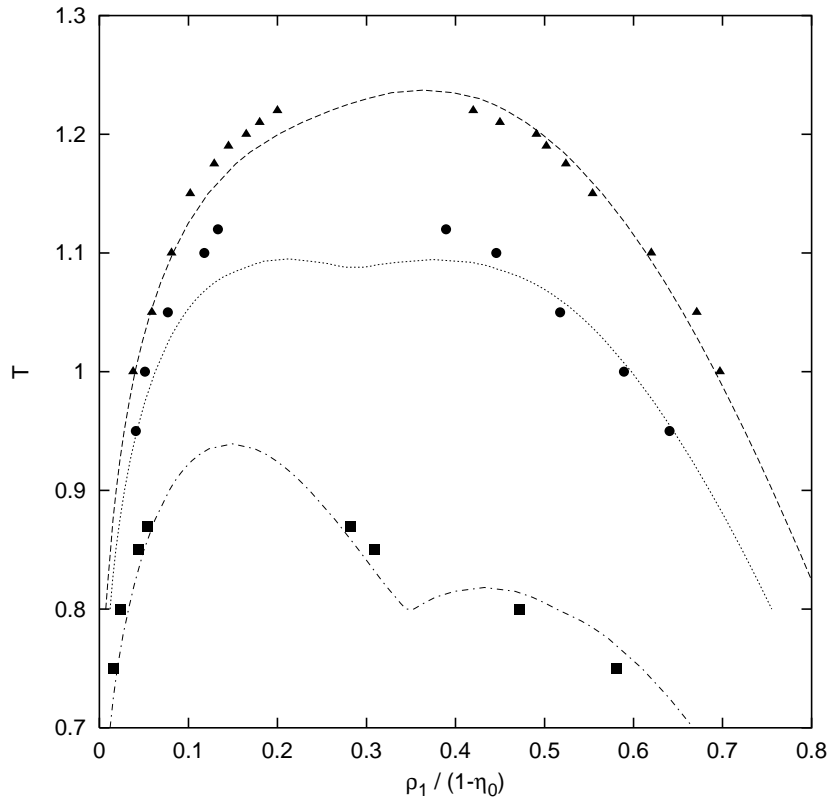


FIG. 3. Comparison of the coexistence envelopes for a fluid confined in purely repulsive ($y = 0$) equilibrium hard-sphere matrices ($\rho_0 = 0$ (bulk), 0.046 and 0.15 from top to bottom) obtained by computer simulations (symbols) [27] and within the ORPA+B2 (lines) [11].

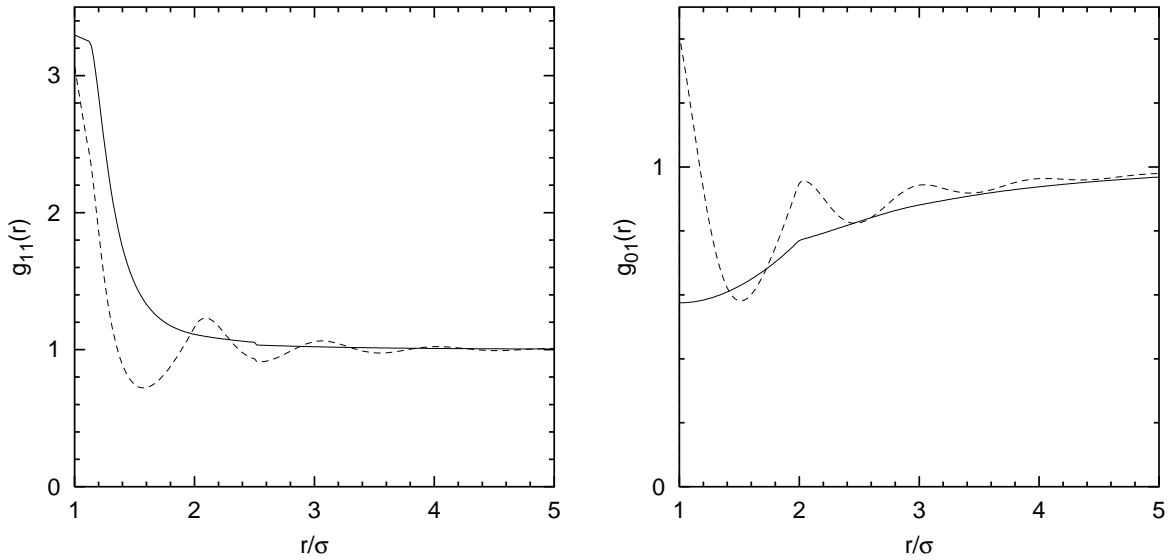


FIG. 4. Fluid-fluid distribution function $g_{11}(r)$ and matrix-fluid distribution function $g_{01}(r)$ calculated with the EXP approximation in an aerogel matrix with $\rho_0 = 0.05$ and $y = 0$ at $T = 0.9$. Solid line: $\rho_1 = 0.02$; dashed line: $\rho_1 = 0.70$.

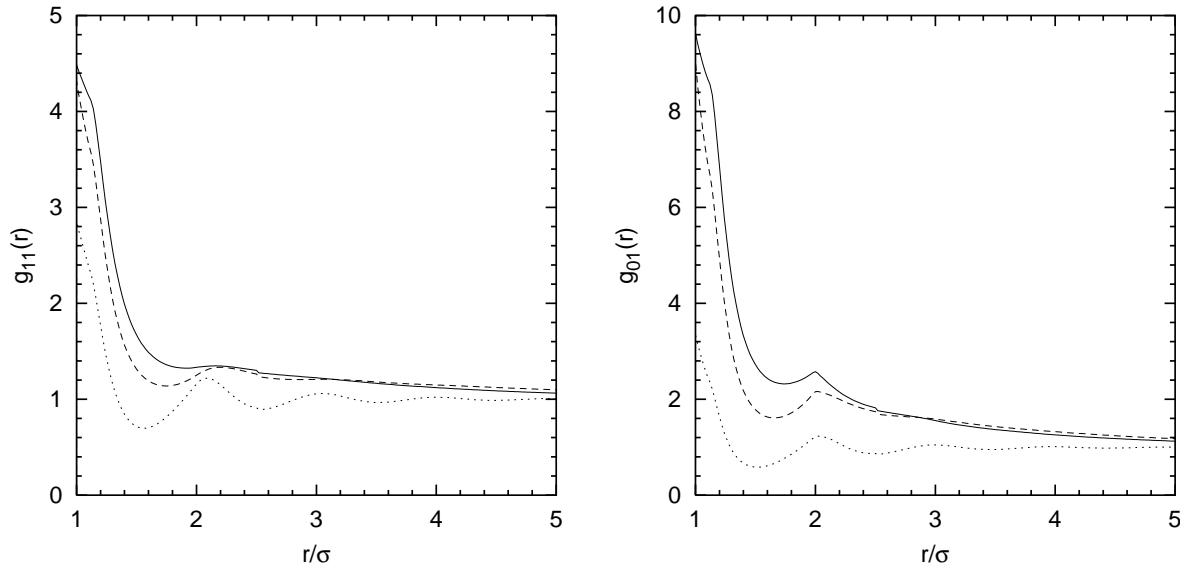


FIG. 5. Fluid-fluid distribution function $g_{11}(r)$ and matrix-fluid distribution function $g_{01}(r)$ calculated with the EXP approximation in an aerogel matrix with $\rho_0 = 0.05$ and $y = 1.5$ at $T = 0.9$. Solid line: $\rho_1 = 0.02$; dashed line: $\rho_1 = 0.2$; dotted line: $\rho_1 = 0.72$.

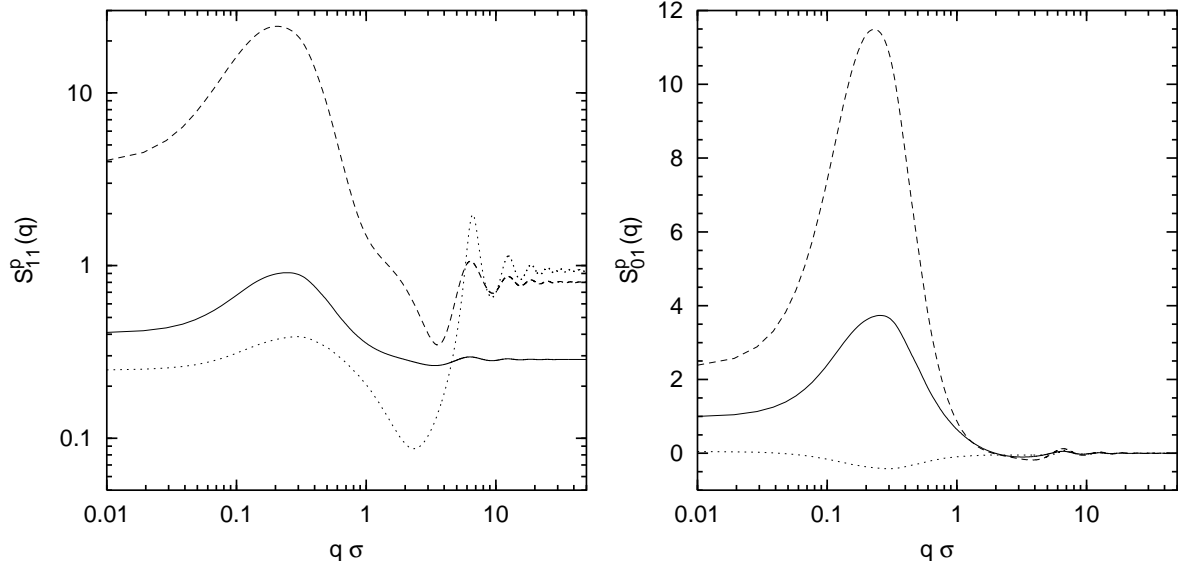


FIG. 6. Partial fluid-fluid structure factor $S_{11}^p(q)$ and matrix-fluid structure factor $S_{01}^p(q)$ calculated within the EXP approximation in an aerogel matrix with $\rho_0 = 0.05$ and $y = 1.5$ at $T = 0.9$. Solid line: $\rho_1 = 0.02$; dashed line: $\rho_1 = 0.2$; dotted line: $\rho_1 = 0.72$. Note that the oscillations of $S_{01}^p(q)$ around zero at large q prevent us from using a logarithmic scale for $S_{01}^p(q)$.

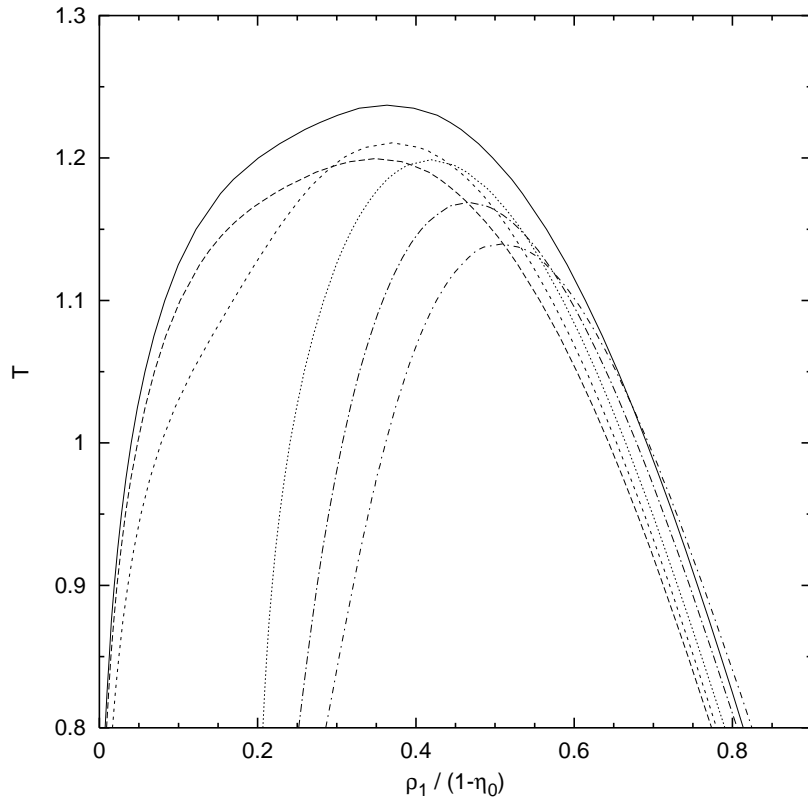


FIG. 7. ORPA+B2 predictions for the coexistence envelopes of the fluid phases in an aerogel matrix with density $\rho_0 = 0.05$. From left to right: $y = 0.5, 1.0, 1.5, 2.0, 2.5$. The solid line is for the bulk fluid.

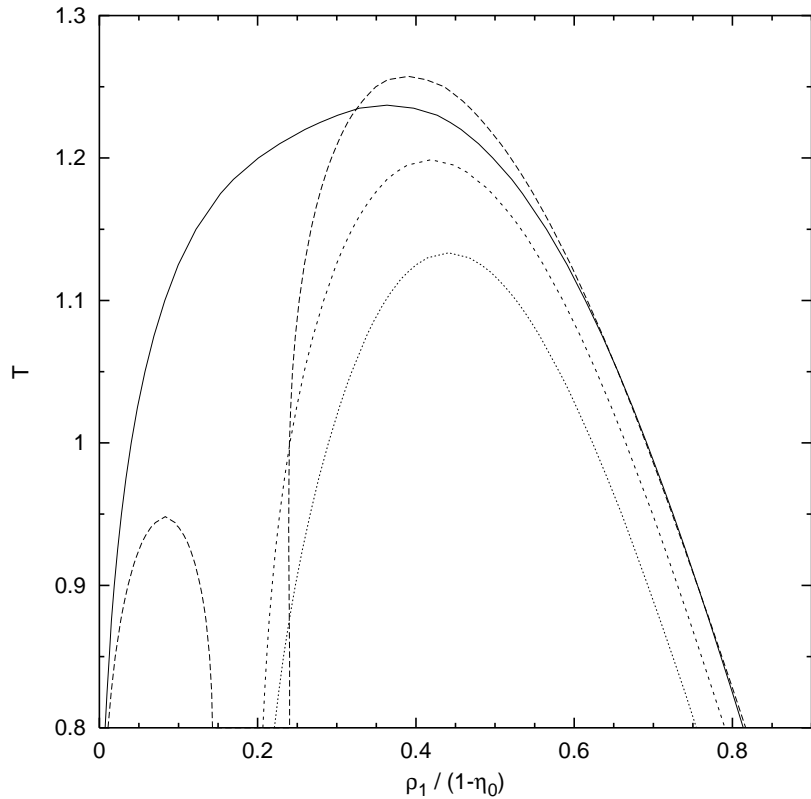


FIG. 8. ORPA+B2 predictions for the coexistence envelopes of the fluid phases in an aerogel matrix with interaction ratio $y = 1.5$. From top to bottom, $\rho_0 = 0.025, 0.05, 0.1$. The solid line is for the bulk fluid.

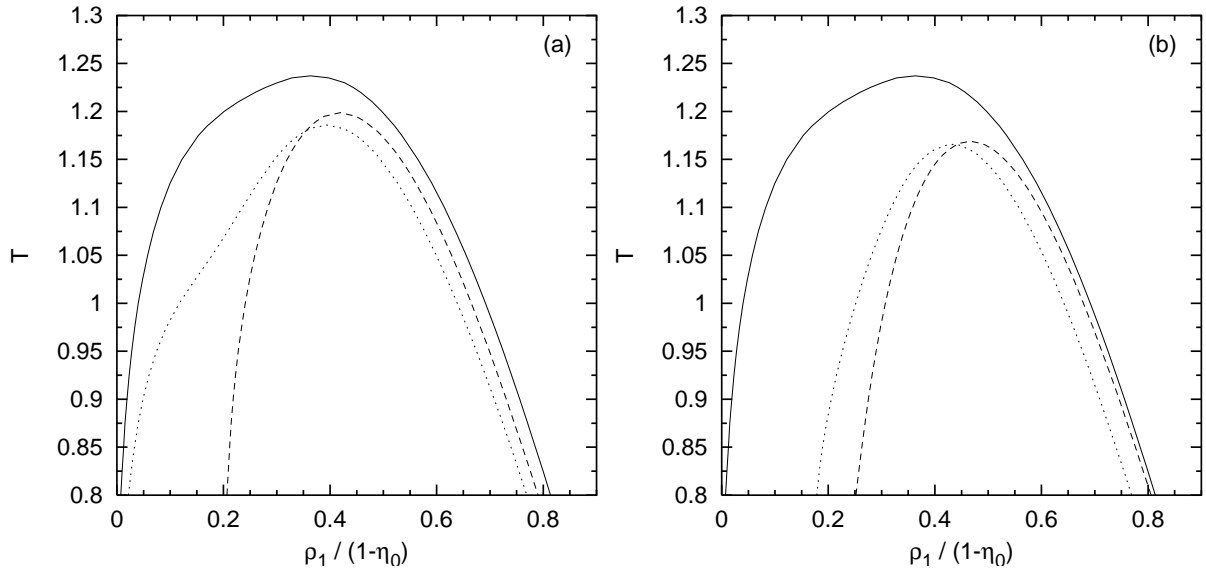


FIG. 9. Comparison of the gas-liquid coexistence envelopes predicted by ORPA+B2 in an equilibrium hard-sphere matrix and a DLCA aerogel at the same matrix density $\rho_0 = 0.05$. (a) $y = 1.5$. Dotted line: hard-sphere matrix; dashed line: aerogel. (b) $y = 2$. Dotted line: hard-sphere matrix; dashed line: aerogel. The solid line is for the bulk fluid.